

Electronic Supporting Information (ESI)

A Linear Metal-Metal Bonded Tri-Iron Single-Molecule Magnet

Table of Contents

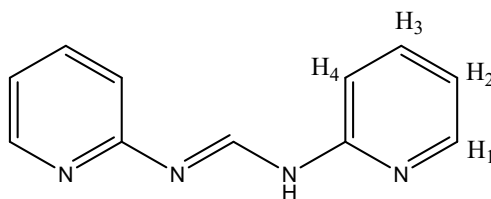
| | |
|-----------------------|----|
| Synthesis | 1 |
| Crystallography | 2 |
| Shape analysis | 4 |
| Calculations | 4 |
| Magnetic Measurements | 6 |
| References | 10 |

Synthesis

Materials. All reactions were carried out under an inert atmosphere of argon or nitrogen using Schlenk and drybox methods. Anhydrous FeCl₂ was purchased from Fisher Chemicals and stored in an oven at 120°C for several days before use. 2-aminopyridine, triethyl-orthoformate and methyllithium (1.6 M in diethylether) were purchased from Sigma Aldrich and used as received. Tetrahydrofuran (THF), diethyl ether (Et₂O), acetonitrile (CH₃CN) and dichloromethane (CH₂Cl₂) were purified using an Innovative Technologies solvent purification system. CDCl₃ was purchased from Eurisotop and used as received. TIBF₄ was synthesized through salt metathesis from the mixture of Tl₂CO₃ and HBF₄ with subsequent drying in vacuo. *Warning: MeLi is pyrophoric and Tl salts are fatal if swallowed.*

Physico-chemical characterization. Elemental analysis was carried out by the Service d'Analyse Élémentaire of the University of Lorraine, Nancy, France. IR spectra were measured on Nicolet 6700 FT-IR using a Smart iTR accessory between 450-4000 cm⁻¹.

HDpyF. 2-aminopyridine (10 g, 0.10 mol) and triethyl-orthoformate (16.7 mL, 14.9 g, 0.10 mol) were refluxed at 150°C for 16 hours under a stream of argon. After cooling, a pale-yellow crystalline material was obtained along with a yellow liquid. The solid was isolated by filtration, recrystallized using a 1:1 mixture of toluene and petroleum ether, and dried for two days at 10⁻⁴–10⁻⁵ mbar to remove traces of water. Yield: 8 g (81%), ¹H NMR (δ/ppm, CDCl₃): 6.98 (broad, H₄); 7.25 (t, H₂); 7.61 (t, H₃); 8.33 (d, H₁); 8.55 (H_{CH}); 9.49 (H_{NH}).



[Fe₃(DpyF)₄](BF₄)₂·2MeCN. A Schlenk flask was charged with HDpyF (0.50 g, 2.5 mmol) and 35 mL of THF. The ligand was deprotonated with MeLi (1.6 M, 1.8 mL, 2.88 mmol) using an acetone-liquid nitrogen bath at -95°C . The resulting golden yellow solution was allowed to warm to room temperature with stirring for 30 minutes. The solution was cannulated into a flask containing anhydrous FeCl₂ (0.24 g, 1.89 mmol) and TIBF₄ (1.10 g 3.78 mmol). A brown suspension was formed within 15 minutes. After the solution was refluxed for 3 hours, a pale-yellow solid was obtained along with a golden-yellow solution. The solvent was removed via filtration and the solid was washed with DCM (2 × 20 mL) and extracted with acetonitrile (20 mL). Golden crystals were obtained within 3 days from the slow diffusion of diethyl ether into the acetonitrile solution. Yield: 0.54 g (61%). Due to facile loss of acetonitrile from crystalline [Fe₃(DpyF)₄](BF₄)₂·2MeCN, samples for elemental analysis were dried under high vacuum for 16 h. One molecule of adventitious water is accounted for in the analysis: Anal. calc. for C₄₄H₃₆Fe₃N₁₆B₂F₈·H₂O: C, 46.03; H, 3.34; N, 19.52%. Found: C, 45.58; H, 3.60; N, 19.95%. FTIR ($\bar{\nu}$, cm⁻¹): 2249w, 1593s, 1536s, 1495w, 1469s, 1434s, 1396w, 1346m, 1315m, 1298m, 1233m, 1159s, 1188w, 1035br, s, 1010m, 945s, 827w, 775s, 738m, 681w, 644s, 563w, 556w.

Crystallography

Single crystals suitable for X-ray diffraction were selected under immersion oil in ambient conditions and attached to a MiTeGen microloop. The crystals were mounted and centered in the X-ray beam using a video camera. Data collection was performed on a Bruker APEXII Quasar diffractometer with Mo K α ($\lambda = 0.71073 \text{ \AA}$) radiation at both 270 and 100 K. The data were collected using a routine to survey reciprocal space, and were reduced and integrated using SAINT⁺¹ and an absorption correction was applied using SADABS.² The structures were solved using direct methods³ and refined by least-squares refinement on F^2 followed by difference Fourier synthesis using Olex2.⁴ All hydrogen atoms were introduced at idealized positions and were allowed to ride on the neighboring atoms with relative isotropic displacement coefficients.

Neither the BF₄⁻ anions or the solvent molecules could be successfully modelled. The solvent molecules could not be located in the difference map, while the boron atoms are on special positions giving rise to octahedral geometries, which could not be modeled as tetrafluoroborate. Modelling as

hexafluorophosphate or hexafluorosilicate was also unsuccessful. Therefore, refinement was done including a solvent mask in Olex2, which calculated a void space of 1702.9 Å³ with 510.9 electrons at 270 K and 1591.1 Å³ with 528.6 electrons at 100 K. This is consistent with the presence of eight BF₄ anions (42 x 8 = 336 electrons), and eight acetonitrile molecules (22 x 8 = 176) electrons, for a total of 512 electrons giving a formula of [Fe(DpyF)₄](BF₄)₂·2CH₃CN.

Table S1. Crystal data and structure refinement for [Fe₃(DpyF)₄](BF₄)₂·2MeCN at 270 and 100 K.

| | | |
|--|--|--|
| Empirical formula | C ₄₄ N ₁₆ Fe ₃ H ₃₆ | C ₄₄ N ₁₆ Fe ₃ H ₃₆ |
| Formula weight | 956.42 | 956.42 |
| Temperature /K | 270(2) | 100(2) |
| Crystal system | tetragonal | tetragonal |
| Space group | <i>I4/m</i> | <i>I4/m</i> |
| <i>a</i> /Å | 12.8314(5) | 12.7015(10) |
| <i>b</i> /Å | 12.8314(5) | 12.7015(10) |
| <i>c</i> /Å | 32.4133(14) | 32.268(3) |
| α /° | 90 | 90 |
| β /° | 90 | 90 |
| γ /° | 90 | 90 |
| Volume/Å ³ | 5336.7(4) | 5205.8(7) |
| <i>Z</i> | 4 | 4 |
| ρ_{calc} g/cm ³ | 1.1903 | 1.2202 |
| μ /mm ⁻¹ | 0.848 | 0.869 |
| <i>F</i> (000) | 1964.7 | 1964.7 |
| Crystal size /mm ³ | 0.089 × 0.085 × 0.023 | 0.056 × 0.02 × 0.02 |
| Radiation | Mo K α (λ = 0.71073) | Mo K α (λ = 0.71073) |
| 2 θ range for data collection /° | 3.42 to 50.76 | 3.44 to 52.96 |
| Index ranges | -15 ≤ <i>h</i> ≤ 15, -15 ≤ <i>k</i> ≤ 15, -39 ≤ <i>l</i> ≤ 39 | -15 ≤ <i>h</i> ≤ 15, -15 ≤ <i>k</i> ≤ 15, -40 ≤ <i>l</i> ≤ 40 |
| Reflections collected | 46155 | 40554 |
| Independent reflections | 2509 [<i>R</i> _{int} = 0.0535, <i>R</i> _{sigma} = 0.0196] | 2750 [<i>R</i> _{int} = 0.0856, <i>R</i> _{sigma} = 0.0367] |
| Data/restraints/parameters | 2509/0/143 | 2750/0/143 |
| Goodness-of-fit on <i>F</i> ² | 1.126 | 1.066 |
| Final <i>R</i> indexes [<i>I</i> ≥ 2 σ (<i>I</i>)] | <i>R</i> ₁ = 0.0352, <i>wR</i> ₂ = 0.1008 | <i>R</i> ₁ = 0.0417, <i>wR</i> ₂ = 0.1134 |
| Final <i>R</i> indexes [all data] | <i>R</i> ₁ = 0.0515, <i>wR</i> ₂ = 0.1199 | <i>R</i> ₁ = 0.0629, <i>wR</i> ₂ = 0.1317 |
| Largest diff. peak/hole / e Å ⁻³ | 0.73/-0.36 | 1.17/-0.51 |

Note: BF₄ anions and solvent molecules were removed from the refinement using the Olex solvent mask.

Table S2. Selected bond Lengths (Å) for [Fe₃(DpyF)₄](BF₄)₂·2MeCN at 270 and 100 K.

| | | 270 K | 100 K |
|-----|-----|------------|------------|
| Fe2 | Fe1 | 2.7839(5) | 2.7742(6) |
| Fe1 | N1 | 2.1511(19) | 2.1479(19) |
| Fe1 | N3 | 2.226(2) | 2.220(2) |
| Fe1 | N4 | 2.196(2) | 2.206(2) |
| Fe2 | N2 | 2.1463(18) | 2.1431(18) |

Shape Analysis

Shape analysis⁵ was carried out using the atomic positions for the Fe(II) center and the (six or four) nitrogen atoms in the first coordination sphere.

Table S3. Continuous shape measure for the terminal Fe(II) atoms in [Fe₃(DpyF)₄](BF₄)₂·2MeCN. Ideal geometry is a zero value, distortion from this geometry increases the value of the continuous shape measures.

| | HP-6 | PPY-6 | OC-6 | TRP-6 | JPPY-6 |
|--------|-------------|--------------|-------------|----------------|---------------|
| Fe(1) | 24.664 | 22.740 | 5.100 | 12.612 | 26.074 |
| Fe(1)' | 24.658 | 22.752 | 5.105 | 12.616 | 26.085 |
| | SP-4 | T-4 | SS-4 | vtBPY-4 | |
| Fe(2) | 3.216 | 17.772 | 9.374 | 20.314 | |

* HP-6: hexagon (D_{6h}); PPY-6: pentagonal pyramid (C_{5v}); OC-6: octahedron (O_h); TRP-6: trigonal prism (D_{3h}); JPPY-6: Johnson pentagonal pyramid J2(C_{5v}), SP-4: square planar (D_{4h}); T-4: tetrahedron (T_d); SS-4: seesaw (C_{2v}); vtBPY-4: vacant trigonal bipyramid (C_{3v}).

Calculations

All calculations described in this paper were performed with version 4.2.1 of the ORCA programme package.⁶ Cartesian coordinates for the D2d-symmetrised geometry used in all calculations is given in **Table S4**. The calculations described in the main text were done using the B3LYP hybrid functional⁷ with 20% Hartree-Fock exchange. Parallel calculations reported here in the supporting information used two alternative hybrids, PBE0⁸ and the meta-hybrid TPSSH.⁹ The precise values of the exchange coupling constant, *J*, shown in **Table S5** differ slightly between functionals but the qualitative description of the ferromagnetic ground state does not. In all cases the def2-TZP basis was used on the Fe centres and def2-SV(P) on all other atoms. The Heisenberg exchange coupling constant, *J*, was extracted from the energies of the ferromagnetic and broken-symmetry states using the formula proposed by Yamaguchi.¹⁰

$$\hat{H} = -2J(\hat{S}_{Fe1}\hat{S}_{Fe2} + \hat{S}_{Fe2}\hat{S}_{Fe3})$$

$$J = -\frac{E_{S_T=6} - E_{M_S=2}}{\langle S^2 \rangle_{S_T=6} - \langle S^2 \rangle_{M_S=2}}$$

Table S4. D_{2d} -symmetrised Cartesian coordinates using in the calculations.

| | | | | | | | |
|----|--------------|-------------|--------------|---|--------------|--------------|--------------|
| Fe | 0.00000000 | 0.00000000 | 2.78384900 | H | -1.060571714 | 1.060571714 | 6.071336000 |
| Fe | 0.00000000 | 0.00000000 | -2.783849000 | N | 1.444660753 | -1.444660753 | 1.899094500 |
| Fe | 0.00000000 | 0.00000000 | 0.000000000 | N | 1.233568643 | -1.233568643 | 4.117785500 |
| N | 1.519419270 | 1.519419270 | 2.700352500 | N | -1.519419270 | -1.519419270 | 2.700352500 |
| N | -1.519419270 | 1.519419270 | -2.700352500 | N | 1.519419270 | -1.519419270 | -2.700352500 |
| N | 1.492615198 | 1.492615198 | 0.384098000 | N | -1.233568643 | -1.233568643 | -4.117785500 |
| N | -1.492615198 | 1.492615198 | -0.384098000 | N | -1.444660753 | -1.444660753 | -1.899094500 |
| N | 1.444660753 | 1.444660753 | -1.899094500 | N | 1.492615198 | -1.492615198 | -0.384098000 |
| N | -1.444660753 | 1.444660753 | 1.899094500 | N | -1.492615198 | -1.492615198 | 0.384098000 |
| N | 1.233568643 | 1.233568643 | -4.117785500 | C | 1.929901583 | -1.929901583 | 0.790236000 |
| N | -1.233568643 | 1.233568643 | 4.117785500 | C | 1.887708916 | -1.887708916 | 3.145711000 |
| C | 1.978468358 | 1.978468358 | 3.877278500 | C | 1.514152644 | -1.514152644 | 5.399407000 |
| C | -1.978468358 | 1.978468358 | -3.877278500 | C | -2.021790553 | -2.021790553 | 1.553244500 |
| H | 1.621085914 | 1.621085914 | 4.658114500 | C | -1.978468358 | -1.978468358 | 3.877278500 |
| H | -1.621085914 | 1.621085914 | -4.658114500 | C | 1.978468358 | -1.978468358 | -3.877278500 |
| C | 2.948729935 | 2.948729935 | 3.989753000 | C | 2.021790553 | -2.021790553 | -1.553244500 |
| C | -2.948729935 | 2.948729935 | -3.989753000 | C | -1.514152644 | -1.514152644 | -5.399407000 |
| H | 3.243188219 | 3.243188219 | 4.821154000 | C | -1.887708916 | -1.887708916 | -3.145711000 |
| H | -3.243188219 | 3.243188219 | -4.821154000 | C | -1.929901583 | -1.929901583 | -0.790236000 |
| C | 3.459957172 | 3.459957172 | 2.840052500 | H | 2.587068833 | -2.587068833 | 0.822325500 |
| C | -3.459957172 | 3.459957172 | -2.840052500 | C | 2.850121246 | -2.850121246 | 3.445534000 |
| H | 4.116487230 | 4.116487230 | 2.882191000 | C | 2.453933896 | -2.453933896 | 5.747850000 |
| H | -4.116487230 | 4.116487230 | -2.882191000 | H | 1.060571714 | -1.060571714 | 6.071336000 |
| C | 3.019202541 | 3.019202541 | 1.613858000 | C | -3.019202541 | -3.019202541 | 1.613858000 |
| C | -3.019202541 | 3.019202541 | -1.613858000 | H | -1.621085914 | -1.621085914 | 4.658114500 |
| H | 3.374622531 | 3.374622531 | 0.832049000 | C | -2.948729935 | -2.948729935 | 3.989753000 |
| H | -3.374622531 | 3.374622531 | -0.832049000 | C | 2.948729935 | -2.948729935 | -3.989753000 |
| C | 2.021790553 | 2.021790553 | 1.553244500 | H | 1.621085914 | -1.621085914 | -4.658114500 |
| C | -2.021790553 | 2.021790553 | -1.553244500 | C | 3.019202541 | -3.019202541 | -1.613858000 |
| C | 1.929901583 | 1.929901583 | -0.790236000 | H | -1.060571714 | -1.060571714 | -6.071336000 |
| C | -1.929901583 | 1.929901583 | 0.790236000 | C | -2.453933896 | -2.453933896 | -5.747850000 |
| H | 2.587068833 | 2.587068833 | -0.822325500 | C | -2.850121246 | -2.850121246 | -3.445534000 |
| H | -2.587068833 | 2.587068833 | 0.822325500 | H | -2.587068833 | -2.587068833 | -0.822325500 |
| C | 1.887708916 | 1.887708916 | -3.145711000 | H | 3.299494688 | -3.299494688 | 2.769068000 |
| C | -1.887708916 | 1.887708916 | 3.145711000 | C | 3.114270767 | -3.114270767 | 4.767348000 |
| C | 2.850121246 | 2.850121246 | -3.445534000 | H | 2.633909371 | -2.633909371 | 6.642133000 |
| C | -2.850121246 | 2.850121246 | 3.445534000 | H | -3.374622531 | -3.374622531 | 0.832049000 |
| H | 3.299494688 | 3.299494688 | -2.769068000 | C | -3.459957172 | -3.459957172 | 2.840052500 |
| H | -3.299494688 | 3.299494688 | 2.769068000 | H | -3.243188219 | -3.243188219 | 4.821154000 |
| C | 3.114270767 | 3.114270767 | -4.767348000 | H | 3.243188219 | -3.243188219 | -4.821154000 |
| C | -3.114270767 | 3.114270767 | 4.767348000 | C | 3.459957172 | -3.459957172 | -2.840052500 |
| H | 3.750821652 | 3.750821652 | -4.992297000 | H | 3.374622531 | -3.374622531 | -0.832049000 |
| H | -3.750821652 | 3.750821652 | 4.992297000 | H | -2.633909371 | -2.633909371 | -6.642133000 |
| C | 2.453933896 | 2.453933896 | -5.747850000 | C | -3.114270767 | -3.114270767 | -4.767348000 |
| C | -2.453933896 | 2.453933896 | 5.747850000 | H | -3.299494688 | -3.299494688 | -2.769068000 |
| H | 2.633909371 | 2.633909371 | -6.642133000 | H | 3.750821652 | -3.750821652 | 4.992297000 |
| H | -2.633909371 | 2.633909371 | 6.642133000 | H | -4.116487230 | -4.116487230 | 2.882191000 |
| C | 1.514152644 | 1.514152644 | -5.399407000 | H | 4.116487230 | -4.116487230 | -2.882191000 |
| C | -1.514152644 | 1.514152644 | 5.399407000 | H | -3.750821652 | -3.750821652 | -4.992297000 |
| H | 1.060571714 | 1.060571714 | -6.071336000 | | | | |

Table S5. Calculated energies, spin densities, values of $\langle S^2 \rangle$ and exchange coupling constants, J , using three different hybrid functionals.

| | | E / eV | $\rho(\text{Fe1})$ | $\rho(\text{Fe2})$ | $\rho(\text{Fe3})$ | $\langle S^2 \rangle$ | $J/k_B / \text{K}$ |
|-------|-----------|-----------------|--------------------|--------------------|--------------------|-----------------------|--------------------|
| B3LYP | $S = 6$ | -173089.64 | 3.78 | 3.66 | 3.78 | 42.05 | 43.2 |
| | $M_S = 2$ | -173089.40 | 3.73 | -3.83 | 3.73 | 10.03 | |
| PBE0 | $S = 6$ | -173039.44 | 3.83 | 3.72 | 3.83 | 42.05 | 34.2 |
| | $M_S = 2$ | -173039.25 | 3.80 | -3.89 | 3.80 | 10.03 | |
| TPSSH | $S = 6$ | -173145.46 | 3.80 | 3.65 | 3.80 | 42.05 | 52.2 |
| | $M_S = 2$ | -173145.17 | 3.72 | -3.85 | 3.72 | 10.02 | |

Magnetic Measurements

Magnetic susceptibility measurements were performed on a Quantum Design SQUID MPMS-XL magnetometer and PPMS-9 susceptometer housed at the Centre de Recherche Paul Pascal at temperatures between 1.8 and 300 K and dc magnetic fields ranging from -7 to $+7$ T. The ac magnetic susceptibility measurements were performed in an oscillating ac field of 1 to 10 Oe with frequencies between 10 and 10000 Hz and various dc fields (including zero). The measurements were carried out on a freshly-filtered polycrystalline samples of $[\text{Fe}_3(\text{DpyF})_4](\text{BF}_4)_2 \cdot 2\text{MeCN}$ (9.8 and 14.0 mg) suspended in mineral oil (14.6, 17.4 mg) and introduced in a sealed polyethylene bag ($3 \times 0.5 \times 0.02$ cm; 30 and 19.8 mg). Prior to the experiments, the field-dependent magnetization was measured at 100 K on each sample to exclude the presence of bulk ferromagnetic impurities. In fact, paramagnetic or diamagnetic materials should exhibit a perfectly linear dependence of the magnetization that extrapolates to zero at zero dc field; the samples appeared to be free of any ferromagnetic impurities. The magnetic susceptibilities were corrected for the sample holder, the mineral oil and the intrinsic diamagnetic contributions.

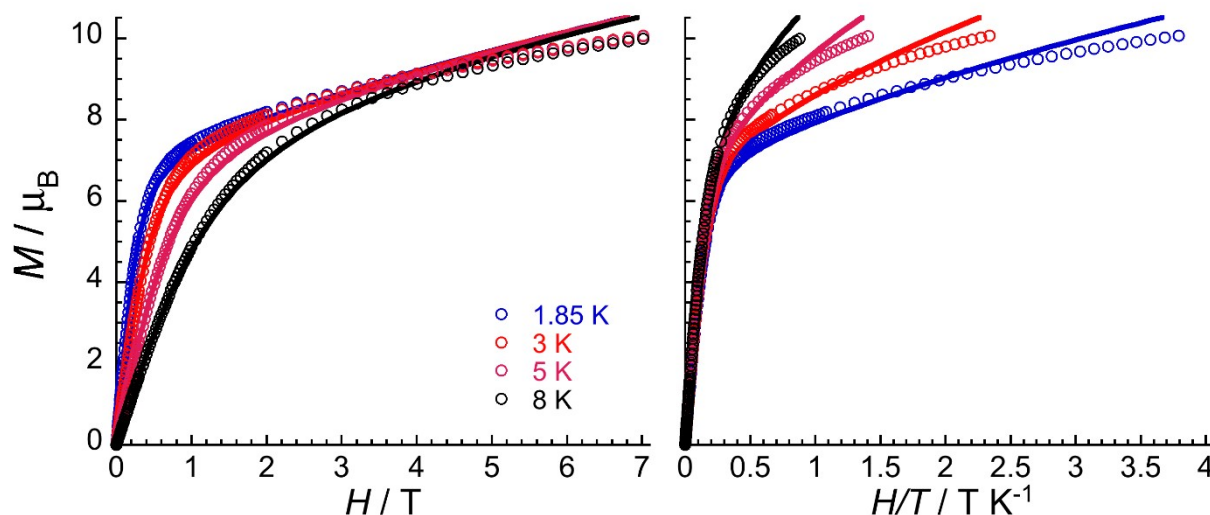


Figure S1. Field dependence of the magnetization, M , for $[\text{Fe}_3(\text{DpyF})_4](\text{BF}_4)_2 \cdot 2\text{MeCN}$ below 8 K (scanning at $10 - 40 \text{ mT} \cdot \text{min}^{-1}$ for $H < 1 \text{ T}$ and $50 - 250 \text{ mT} \cdot \text{min}^{-1}$ for $H > 1 \text{ T}$) plotted as (left) M vs H and (right) M vs H/T plots. The solid lines are the best fit of the magnetization data to the model described in the main text.

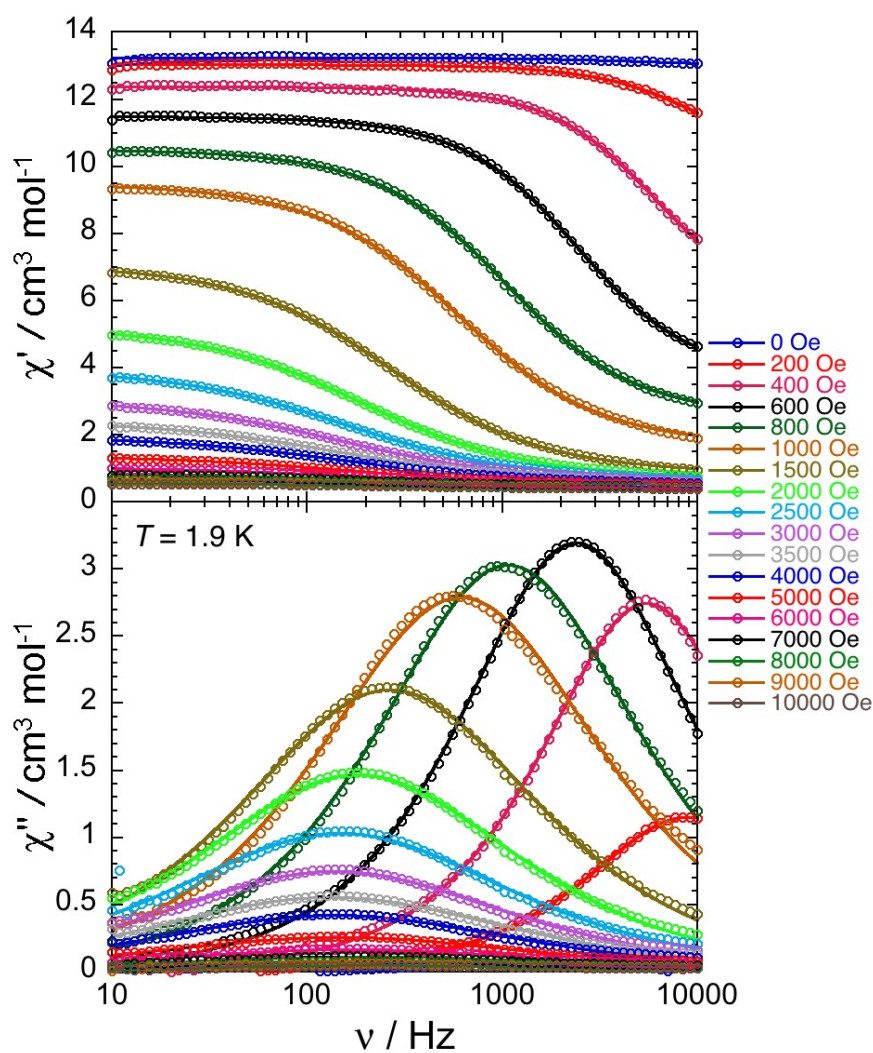


Figure S2. ac frequency dependence of the real (χ' , top) and imaginary (χ'' , bottom) parts of the ac susceptibility for $[\text{Fe}_3(\text{DpyF})_4](\text{BF}_4)_2 \cdot 2\text{MeCN}$, at 1.9 K between 10 and 10000 Hz in dc-field between 0 and 1 T. Solid lines are the generalised Debye fit¹¹ of the ac data used to extract the field dependence of the relaxation time shown in Figure S5.

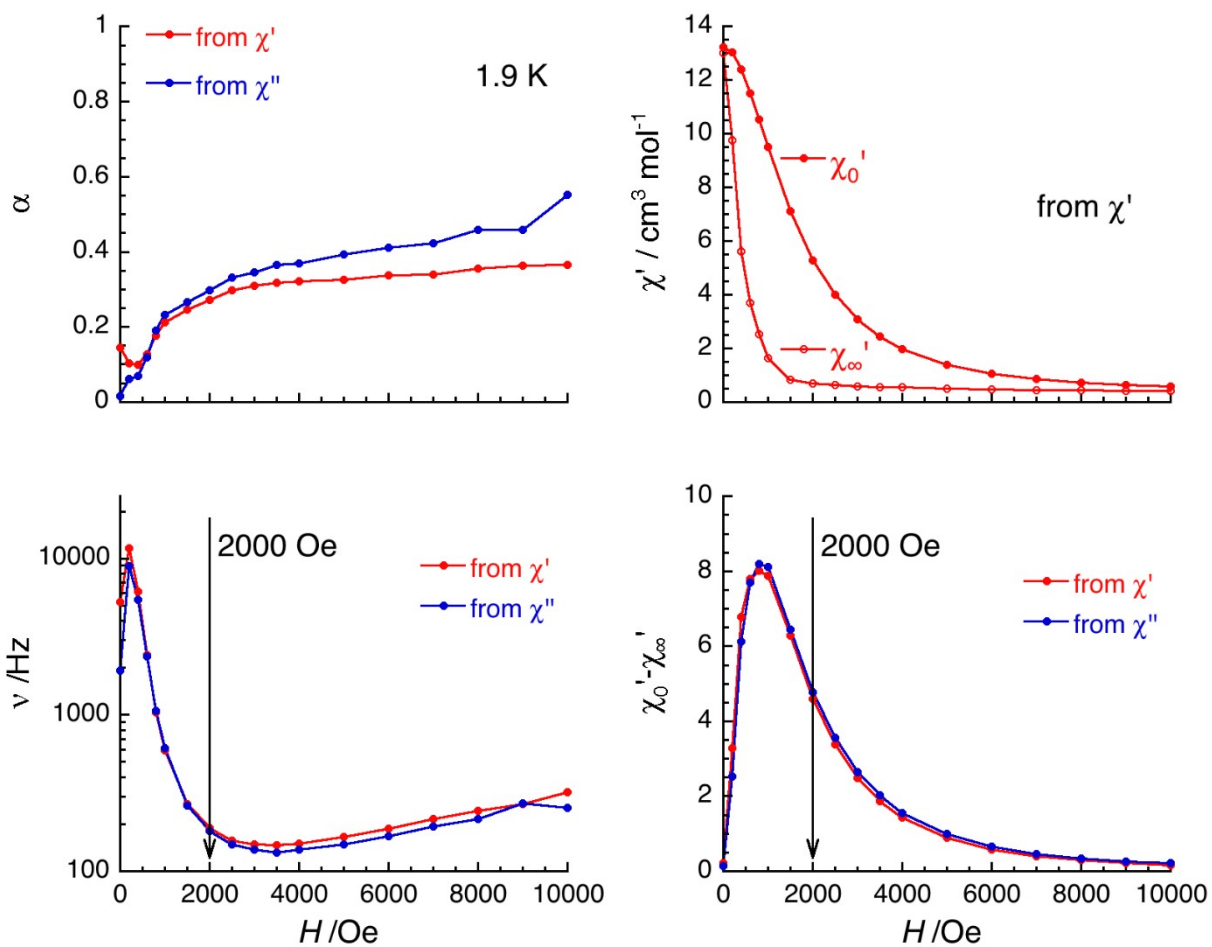


Figure S3. Field dependence of the parameters, α , ν , χ_0' , χ_∞' and $\chi_0' - \chi_\infty'$, between 0 and 1 T at 1.9 K deduced from the generalised Debye fit¹¹ of the frequency dependence of the real (χ') and imaginary (χ'') components of the ac susceptibility shown in Figure S2 for $[\text{Fe}_3(\text{DpyF})_4](\text{BF}_4)_2 \cdot 2\text{MeCN}$.

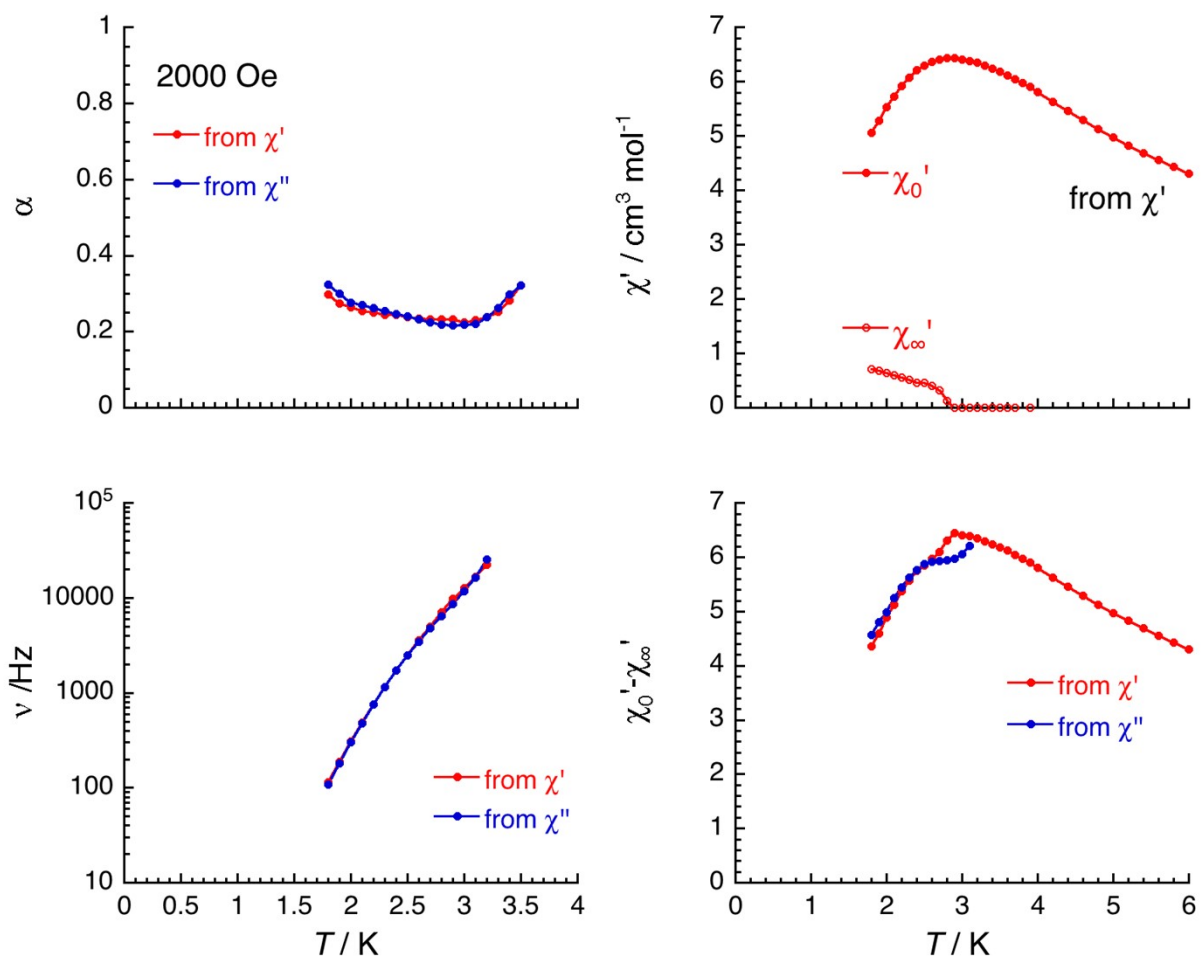


Figure S4. Temperature dependence of the parameters, α , ν , χ_0' , χ_∞' and $\chi_0' - \chi_\infty'$, between 1.85 and 6 K at 2000 Oe deduced from the generalised Debye fit¹¹ of the frequency dependence of the real (χ') and imaginary (χ'') components of the ac susceptibility shown in Figure 4 for $[\text{Fe}_3(\text{DpyF}_4)_4](\text{BF}_4)_2 \cdot 2\text{MeCN}$.

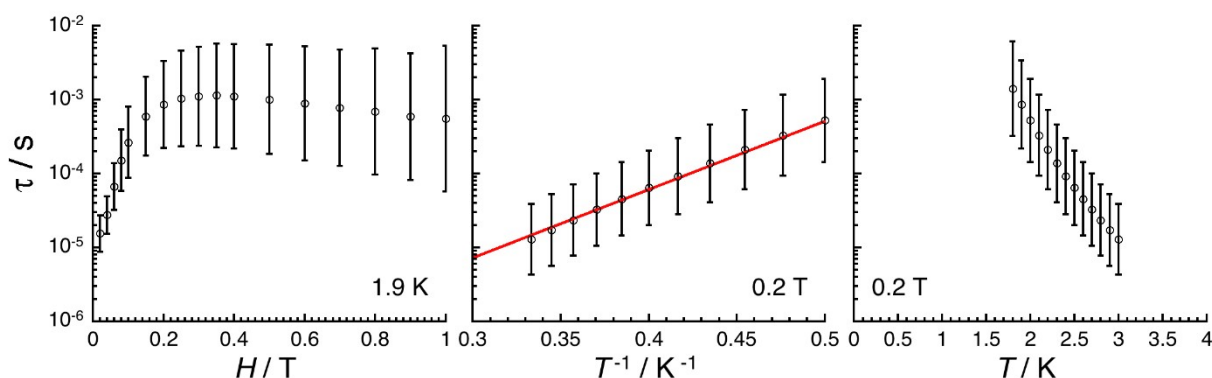


Figure S5. Relaxation time variation for $[\text{Fe}_3(\text{DpyF})_4](\text{BF}_4)_2 \cdot 2\text{MeCN}$ as a function of the applied magnetic field at 1.9 K between 0 and 1 T (left) and as a function of the temperature between 1.8 and 3 K plotted as τ vs. T^{-1} (center) and τ vs. T (right) at 0.2 T dc fields (semi-logarithm plots). The reported relaxation time was estimated from the generalized Debye fits of the ac susceptibility data (Figures S3 and S4) shown in Figures 4 and S2. Estimated standard deviations of the relaxation time (vertical solid bars) have been calculated from the α parameters of the generalized Debye fit (Figures S3 and S4) and the log-normal distribution as described in reference 12. The solid red line is the best fit discussed in the text.

References

1. Bruker APEX2, SAINT+. Bruker AXS Inc., Madison, Wisconsin, USA, 2012.
2. Bruker SADABS, Bruker AXS Inc., Madison, Wisconsin, USA, 2001.
3. Sheldrick, G. M. SHELXL-97: Program for Crystal Structure Refinement; University of Göttingen: Göttingen, Germany, 1997.
4. O. V. Dolomanov, L. J. Bourhis, R. J. Gildea, J. A. K. Howard, H. Puschmann, *J. Appl. Cryst.*, 2009, **42**, 339.
5. *SHAPE. Program for the Stereochemical Analysis of Molecular Fragments by Means of Continuous Shape Measures and Associated Tools*, Barcelona, 2013.
6. F. Neese, Orca 4.2.1: *Wiley Interdisciplinary Reviews: Computational Molecular Science*, 2017, **8**, 1, e1327.
7. P.J. Stephens, P. J.; Devlin, C.F. Chabalowski, M.J. Frisch, *J. Phys. Chem.*, 1994, **98**, 11623.
8. (a) C. Adamo, V. Barone, *J. Chem. Phys.*, 1999, **110**, 6158; (b) J.P. Perdew, A. Ruzsinsky, G.I. Csonka, L.A. Constantin and J. Sun, *Phys. Rev. Lett.*, 2011, **106**, 179902.
9. (a) J. Sun, A. Ruzsinsky, J.P. Perdew, *Phys. Rev. Lett.*, 2015, **115**, 036402; (b) M. Swart, A.W. Ehlers, K. Lammertsma, *Mol. Phys.* 2004, 102, 2467; (c) N.C. Handy, A.J. Cohen, *Mol. Phys.*, 2001, **99**, 403; (d) J.P. Perdew, K. Burke, M. Ernzerhof, *Phys. Rev. Lett.*, 1996, **77**, 3865.
10. (a) K. Yamaguchi Y. Takahara T. Fueno in: V.H. Smith (Ed.), *Applied Quantum Chemistry*. Reidel, Dordrecht, 1986, pp 155-184; (b) T. Soda, Y. Kitagawa, T. Onishi, Y. Takano, Y. Shigeta, H. Nagao, Y. Yoshioka, K. Yamaguchi, *Chem. Phys. Lett.*, 2000, **319**, 223.
11. K. S. Cole, R. H. Cole, *J. Chem. Phys* 1941, **9**, 341.
12. D. Reta, N. F. Chilton, *PCCP*, 2019, **21**, 23567.